

## Enhanced blue-violet emission by inverse energy transfer to the Ge-related oxygen deficiency centers via Er<sup>3+</sup> ions in metal-oxide semiconductor structures

A. Kanjilal,<sup>a)</sup> L. Rebohle, M. Voelskow, W. Skorupa, and M. Helm

*Institute of Ion Beam Physics and Materials Research, Forschungszentrum Dresden-Rossendorf e.V., P.O. Box 51 01 19, 01314 Dresden, Germany*

(Received 1 December 2008; accepted 7 January 2009; published online 4 February 2009)

It is generally believed that the 1.5  $\mu\text{m}$  Er luminescence is enhanced by transferring energy from Si nanocrystals to the nearest Er<sup>3+</sup> ions in Er-doped Si-rich SiO<sub>2</sub> layers during optical pumping. Here, the influence of Ge nanocrystals instead of excess Si in the same environment is studied using electroluminescence technique on metal-oxide-semiconductor structures. An increase of the 400 nm electroluminescence intensity with a concomitant reduction of the Er-related emission is observed. This is explained in the light of an inverse energy transfer process from Er<sup>3+</sup> to the Ge-related oxygen-deficiency centers. © 2009 American Institute of Physics. [DOI: 10.1063/1.3077169]

Recently, Si nanocrystals (NCs) in SiO<sub>2</sub> received much attention, since they can act as *sensitizers* for increasing the intensity of the 1.53  $\mu\text{m}$  Er luminescence in layers codoped with Er ions.<sup>1–4</sup> The natural question arises, whether and/or how this behavior will change by using NCs of Ge, which is chemically very similar to Si. The optoelectronic properties of Ge NCs in SiO<sub>2</sub> have been investigated<sup>5,6</sup> to a much lesser extent than that of Si. The underlying physics behind such light emitting devices (LEDs) has generally been expressed in terms of recombination of charge carriers either in Ge NCs through bandgap opening<sup>7</sup> according to the quantum confinement model<sup>5</sup> or in defect states<sup>6</sup> during electrical/optical pumping. Emission of light at  $\sim 400$  nm has been reported<sup>6</sup> as a result of optical and/or electrical excitation of the Ge-related oxygen-deficiency center (GeODC) into the first singlet state ( $S_1$ ), followed by the intersystem crossing to the first triplet state ( $T_1$ ), and a radiative transition back to the ground singlet state ( $S_0$ ). Recent photoluminescence studies<sup>8,9</sup> revealed that this system could be used for visible range pumping of Er<sup>3+</sup> ions where Ge nanoclusters behave as sensitizers. In fact, the application of such a system in Si-based electronic platform requires the fabrication of a metal-oxide semiconductor (MOS) structure while the electroluminescence (EL) efficiency is crucial for device performance.

In this letter, we present the fabrication of Si-based MOSLEDs where Ge NCs and/or Er<sup>3+</sup> ions are dispersed into the SiO<sub>2</sub> layer. In particular, we demonstrate a pronounced increase in the 400 nm EL intensity by Er-doping with a concomitant reduction in the Er emission, implying an *inverse energy transfer* from Er<sup>3+</sup> to the GeODCs. This is contrary to the phenomenon commonly accepted for Er-doped Si-rich SiO<sub>2</sub> layers where energy is known to transfer from Si NC to the nearby Er<sup>3+</sup> ions,<sup>1–4</sup> keeping in mind the spatial location of the Er sites.<sup>10</sup>

Initially 130 keV Ge ions were implanted at room temperature (RT) with a dose of  $2 \times 10^{16}$  ions/cm<sup>2</sup> into a thermally grown SiO<sub>2</sub> layer of thickness 200 nm on *n*-type (100)Si wafers. The samples were subjected to rapid thermal annealing at 1050 °C for 180 s according to Ref. 11 in nitrogen ambience to produce Ge NCs. Subsequently, 250 keV

Er ions were implanted with a dose of  $1 \times 10^{15}$  ions/cm<sup>2</sup> into the Ge-rich SiO<sub>2</sub> layer, followed by short-time annealing at 1050 °C for 6 s not only to remove ion-beam induced defects, but also to activate Er<sup>3+</sup> ions. Both Ge and Er ions provide Gaussian-like profiles with maximum concentrations of  $\sim 3.5\%$  and  $0.3\%$  at  $R_p$  of  $\sim 112$  and  $115$  nm, respectively. Two reference samples were also prepared by implanting either Ge or Er ions into the SiO<sub>2</sub> layers followed by annealing at 1050 °C for 180 and 6 s, respectively. A semitransparent indium tin oxide and aluminum contacts were sputter deposited in the front and rear surfaces, respectively, to achieve a MOS structure. Circular electrodes with a diameter of 0.2–1.1 mm were subsequently patterned in the front surface by photolithography. The EL spectra were recorded at RT with a single grating monochromator and a photomultiplier, a liquid-nitrogen cooled InGaAs detector, or a charge-coupled device detector. The InGaAs detector or the photomultiplier in combination with a photon counting system were employed to study the time-resolved EL dynamics. Cross-sectional transmission electron microscopy (TEM) images were taken by means of a FEI Titan 80–300 S/TEM.

Formation of Er/Er-oxide clusters with dimension in the range of 2–5 nm (indicated by white arrows) [Fig. 1(a)] in Er-doped SiO<sub>2</sub> layers, called Er:SiO<sub>2</sub>, was seen using high-resolution TEM (HRTEM), while Ge NCs with an in-plane diameter of  $\sim 4$  nm (marked by black arrows) were observed in Ge-rich SiO<sub>2</sub> layers, called Ge-NCs:SiO<sub>2</sub> [Fig. 1(b)]. Although the composition of the clusters in Er:SiO<sub>2</sub> is not yet known, on the basis of the thermodynamic properties of Er and its oxide,<sup>12</sup> we feel that the formation of Er oxide is more favorable than that of Er. However, no specific variation in size and distribution of NC was observed in Er-doped Ge-NCs:SiO<sub>2</sub> layers, named Er:Ge-NCs:SiO<sub>2</sub> [Fig. 1(c)]; the corresponding HRTEM image is displayed in Fig. 1(d).

Figure 2 shows the EL spectra of the Ge-rich MOSLEDs with or without Er ions for a constant current density ( $J$ ) of 0.17 mA/cm<sup>2</sup>. The spectrum for the Er-doped MOSLED is characterized by four EL bands, namely,  $P_1$  to  $P_4$ , in the spectral range between blue violet and infrared, which are assigned as the radiative transitions in Er<sup>3+</sup> from the  $^2H_{11/2}$ ,  $^4S_{3/2}$ ,  $^4F_{9/2}$  and  $^4I_{13/2}$  states to the ground state ( $^4I_{15/2}$ ), respectively.<sup>13</sup> Nevertheless, the Er emission in the short wavelength region, especially the  $^2H_{9/2} \rightarrow ^4I_{15/2}$  transition in-

<sup>a)</sup>Electronic mail: a.kanjilal@fzd.de.

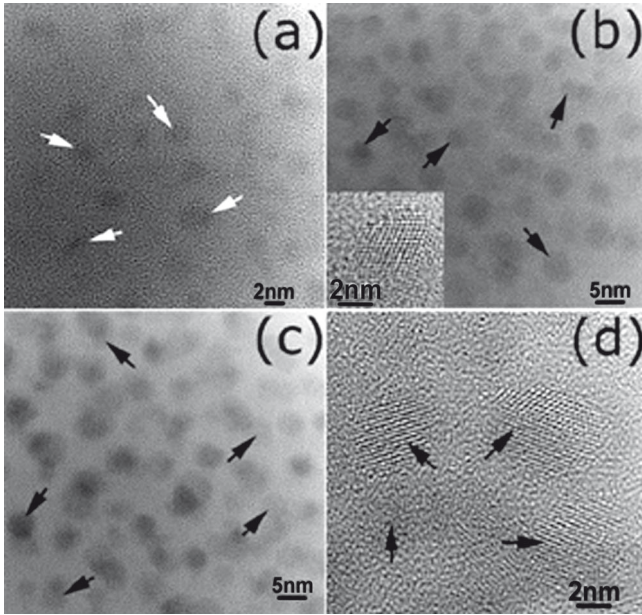


FIG. 1. Bright-field TEM images, with electron beam direction along the [110] zone axis for the (a) Er:SiO<sub>2</sub>, (b) Ge-NCs:SiO<sub>2</sub>, [(c) and (d)] and Er:Ge-NCs:SiO<sub>2</sub> are shown. Inset of (b) displays the HRTEM of a Ge NC of the Ge-NCs:SiO<sub>2</sub>, where crystalline Ge core shows the {111} faceting. HRTEM of the Er:Ge-NCs:SiO<sub>2</sub> (d) depicts randomly oriented Ge-NCs (denoted by black arrows).

duced ~410 nm EL (inset of Fig. 2) can be distinguished for  $J=7.1$  mA/cm<sup>2</sup>. The EL peak of ~400 nm in Ge-NCs:SiO<sub>2</sub> is attributed to the GeODC (as a consequence of the  $T_1 \rightarrow S_0$  transition).<sup>6</sup> Our key result is the increase in the 400 nm EL intensity at the expense of Er-related emission upon Er doping. Quantitative measurements show that the 1532 nm EL yield of the Er<sup>3+</sup> is suppressed by a factor of ~3 in presence of Ge NCs. Whereas other Er EL bands are hardly distinguishable due to the broadening of the 400 nm peak and possible decrease in intensity of those Er emissions by a factor similar to the 1532 nm Er EL.

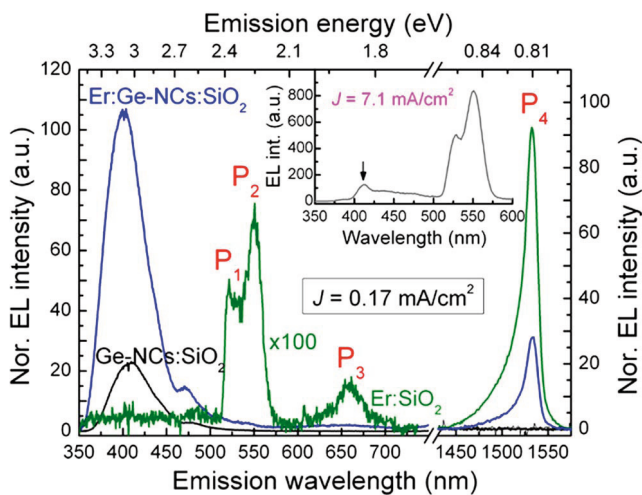


FIG. 2. (Color online) The visible and infrared EL spectra, plotted by solid lines in black, green, and blue for the Ge-NCs:SiO<sub>2</sub>, Er:SiO<sub>2</sub>, and Er:Ge-NCs:SiO<sub>2</sub>, respectively, with  $J=0.17$  mA/cm<sup>2</sup>. Note that the scale given in the left and right ordinates are independent of each other as the signals in the visible and infrared regions were collected by two different detectors. 100 for better projection, where  $P_1$  to  $P_4$  represent radiative transitions from Inset shows an additional EL spectrum for Er:SiO<sub>2</sub> with  $J=7.1$  mA/cm<sup>2</sup>; a prominent peak at ~410 nm is indicated by the downward arrow.

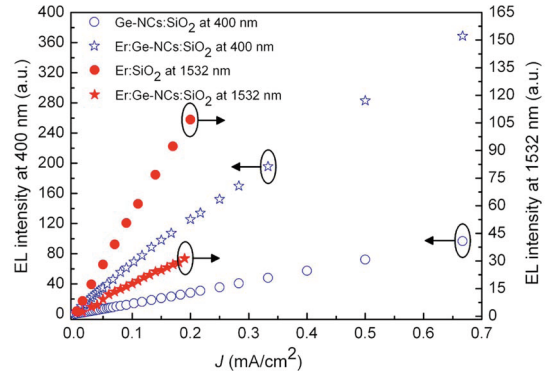


FIG. 3. (Color online) Relative intensities of the 400 nm peak for Ge-NCs:SiO<sub>2</sub> and Er:Ge-NCs:SiO<sub>2</sub> are denoted by blue open circles (○) and blue solid stars (☆), respectively. Similarly, the relative 1532 nm peak intensities for Er:SiO<sub>2</sub> and Er:Ge-NCs:SiO<sub>2</sub> are depicted by red solid circles (●) and red solid stars (★), respectively.

The current-voltage ( $I$ - $V$ ) characteristics of the working devices have also been tested (not shown), confirming that the device integrity is unaffected during device processing; the  $I$ - $V$  profiles can be interpreted in the light of injection of electrons from the conduction band (CB) of the Si to the CB of SiO<sub>2</sub> via the Fowler–Nordheim or trap-assisted tunneling.<sup>14</sup> Furthermore, the 400 and 1532 nm EL intensities are found increasing linearly as a function of  $J$  (Fig. 3), where each of them can be fitted by  $EL(J) = EL_{\max}[\sigma\tau\phi/(\sigma\tau\phi+1)]$ ,<sup>15</sup>  $\phi=J/q$ . The product of the excitation cross section ( $\sigma$ ) and lifetime ( $\tau$ ) for the former peak increases from  $2.3 \times 10^{-20}$  to  $5.4 \times 10^{-17}$  cm<sup>2</sup> s by Er doping, while it varies from  $6.5 \times 10^{-17}$  to  $1.7 \times 10^{-16}$  cm<sup>2</sup> s for the later by incorporating Ge NCs.

It is assumed that during implantation Si and oxygen (O) atoms are released from the SiO<sub>2</sub> network. In the following phases of annealing, displaced O can either be reintegrated into the SiO<sub>2</sub> network or be used in oxidizing implanted element(s), where the formation enthalpies ( $\Delta G_f$ ) of GeO, GeO<sub>2</sub>, SiO<sub>2</sub>, and Er<sub>2</sub>O<sub>3</sub> are  $-237.2$ ,  $-521.4$ ,  $-856.3$ , and  $-1808.7$  kJ/mol, respectively.<sup>12</sup> Indeed, reconstruction of SiO<sub>2</sub> is favorable in Ge implanted SiO<sub>2</sub>, where Ge atoms try to form NCs by Ostwald ripening and eventually triggers the formation of GeODCs near the NC/SiO<sub>2</sub> interface. The Er<sub>2</sub>O<sub>3</sub> configuration is preferable in Er:SiO<sub>2</sub> due to high  $\Delta G_f$  and leads to the formation of Er oxide clusters during annealing [Fig. 1(a)]. We should note here that in contrary to Ref. 16, HRTEM results reveal that Er doping does not give rise to (i) preferential nucleation of amorphous Ge, (ii) fragmentation of NCs by sputtering, (iii) evolution of bigger NCs, or (iv) dissolution of NCs via ion-beam-mixing for Ge-NCs:SiO<sub>2</sub> layers (Fig. 1). Therefore, even if we assume a variation in the cross-section without any change in microstructure, the two independent changes in Fig. 2 (quenching of the 1532 nm Er EL and the rise of the Ge-related 400 nm EL intensity) cannot be interpreted, unless we consider an energy transfer mechanism to the GeODC via Er<sup>3+</sup>, called *inverse energy transfer* process.

The energy levels up to  $^2H_{11/2}$  of an Er<sup>3+</sup> ion lay below the level  $T_1$  of GeODC and hence cannot take part in energy-transfer process. Although the high energy level Er transitions are not evident in case of Er:SiO<sub>2</sub> by using a low  $J$  value (0.17 mA/cm<sup>2</sup>), upon injection of electrons with a moderate  $J$  (~7.1 mA/cm<sup>2</sup>), other Er-related EL peaks, es-

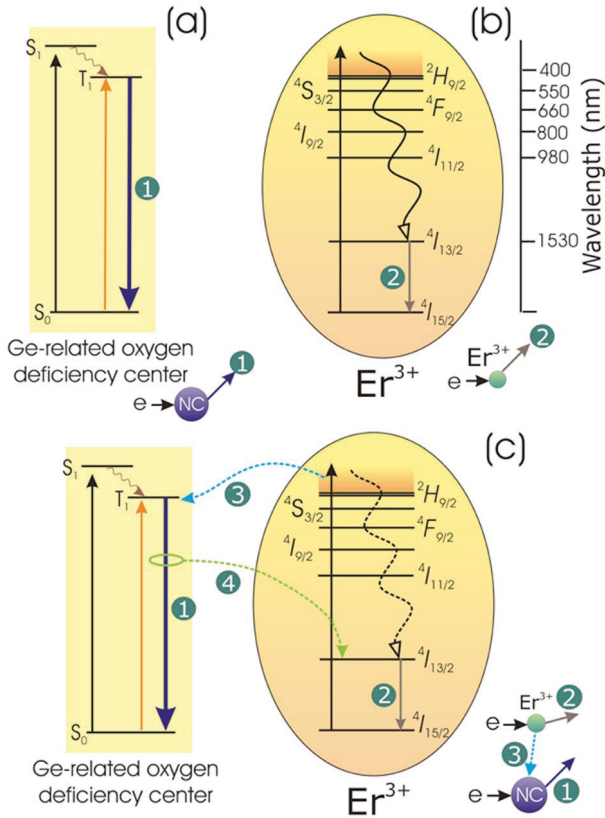


FIG. 4. (Color online) A hot electron excited Ge-related defect center in Ge-NCs:SiO<sub>2</sub> is shown in (a), where the radiative transition from the level  $T_1$  is marked by 1. Electronic excitation of an Er<sup>3+</sup> in Er:SiO<sub>2</sub> is shown in (b), while the downward arrow labeled as 2 represents the infrared emission of Er<sup>3+</sup>. The downward wavy arrow up to  $^4I_{13/2}$  represents a nonradiative transition. Both the radiative defect center and Er<sup>3+</sup> are excited by colliding with hot electrons in Er:Ge-NCs:SiO<sub>2</sub> (c). Here, the downward wavy dashed arrow up to  $^4I_{13/2}$  signifies nonradiative transition, which is either absent or strongly reduced. In all three cases, the corresponding impact-excitation processes are elucidated in the lower right corner of (a)–(c), respectively.

pecially the  $^2H_{9/2} \rightarrow ^4I_{15/2}$  transition mediated  $\sim 410$  nm EL, can be visible (inset of Fig. 2). Clearly, the Er energy levels lying almost in the same height or above than that of  $T_1$  in GeODC [schematically shown in Fig. 4(a)] can contribute to the energy transfer process. For 3.5% of Ge, the 400 nm EL yield reaches its maximum by doping Er up to 0.8%, while the peak intensity quenches by further increase in Er due to concentration quenching.<sup>1</sup> To follow the proposed energy transfer process, the EL lifetime of the Er<sup>3+</sup> excited states has further been examined using a stretched exponential function,<sup>17</sup> which gives  $\tau^{\text{decay}}$  of  $\sim 214$  and  $228$   $\mu\text{s}$  in Er:SiO<sub>2</sub> for the 410 and 550 nm EL, respectively. Because of close proximity, as the 410 nm Er peak is submerged into the Ge-related 400 nm EL intensity in Er:Ge-NCs:SiO<sub>2</sub>, we estimate the corresponding rise ( $\tau^{\text{rise}}$ ) and decay ( $\tau^{\text{decay}}$ ) times for both Ge-NCs:SiO<sub>2</sub> and Er:SiO<sub>2</sub> layers (not shown). While the values of  $\tau^{\text{rise}}$  and  $\tau^{\text{decay}}$  are 46 and 66  $\mu\text{s}$  for the former, the respective values are 27 and 214  $\mu\text{s}$  for the latter. As expected from the energy transfer process, the radiative lifetime of the 400 nm EL hardly changes by Er doping,<sup>2</sup> revealing an increase in  $\sigma$  of the 400 nm EL by an order of three by introducing Er ions.

Based on our results, we believe that the transitions from the  $^2H_{9/2}$  level or above to the ground  $^4I_{15/2}$  level are likely to

be accompanied by a nonradiative relaxation to the lower lying levels of Er<sup>3+</sup> in Er:SiO<sub>2</sub> and as a consequence intensify the green, red, and infrared EL [Fig. 4(b)]. However, the decay time measurements indicate that the Er  $^2H_{9/2}$  level is excited faster than that of the GeODC and can initiate an energy transfer process in Er:Ge-NCs:SiO<sub>2</sub> from Er<sup>3+</sup> to the level  $T_1$  of Ge-related defects (process 3) based on their respective lifetimes [Fig. 4(c)], analogous to the energy back transfer process as reported in Ref. 18. The 1532 nm EL quenching signifies either absence of an additional excitation path from the higher-energy levels to the state  $^4I_{13/2}$  of Er<sup>3+</sup> or excitation of the Er<sup>3+</sup> ions staying apart from Ge NCs. A possible energy back transfer process (process 4) in Fig. 4(c) plays a minor role only.

In summary, we experimentally demonstrated an increase in the Ge-related 400 nm EL intensity at the expense of the Er emission in Er-doped SiO<sub>2</sub> layers containing Ge NCs, showing a strong coupling between the Er<sup>3+</sup> ions and GeODCs. Since the microstructure of the Ge-rich SiO<sub>2</sub> layers is found unaffected by Er doping, based on the decay time measurements, we conclude that an energy transfer from Er<sup>3+</sup> to the triplet state  $T_1$  of the Ge-related defect centers can only justify the observed electroluminescence.

The authors thank J. Schneider and C. Neisser for the ion implantation and sample processing, respectively. The support of the Alexander von Humboldt Foundation is gratefully acknowledged.

- <sup>1</sup>C. Maurizio, F. Iacona, F. D'Acapito, G. Franzò, and F. Priolo, *Phys. Rev. B* **74**, 205428 (2006).
- <sup>2</sup>A. Kanjilal, L. Rebohle, M. Voelskow, W. Skorupa, and M. Helm, *J. Appl. Phys.* **104**, 103522 (2008).
- <sup>3</sup>B. Garrido, C. García, S.-Y. Seo, P. Pellegrino, D. Navarro-Urrios, N. Daldosso, L. Pavesi, F. Gourbilleau, and R. Rizk, *Phys. Rev. B* **76**, 245308 (2007).
- <sup>4</sup>T. Nakamura, M. Fujii, S. Miura, M. Inui, and S. Hayashi, *Phys. Rev. B* **74**, 045302 (2006).
- <sup>5</sup>E. W. H. Kan, W. K. Chim, C. H. Lee, W. K. Choi, and T. H. Ng, *Appl. Phys. Lett.* **85**, 2349 (2004).
- <sup>6</sup>L. Rebohle, J. von Borany, H. Fröb, and W. Skorupa, *Appl. Phys. B: Lasers Opt.* **71**, 131 (2000).
- <sup>7</sup>C. Bulutay, *Phys. Rev. B* **76**, 205321 (2007).
- <sup>8</sup>C. L. Heng, T. G. Finstad, P. Storås, Y. J. Li, and A. E. Gunnæs, *Appl. Phys. Lett.* **85**, 4475 (2004).
- <sup>9</sup>J. S. Jensen, T. P. L. Pedersen, J. Chevallier, B. B. Nielsen, and A. N. Larsen, *Nanotechnology* **17**, 2621 (2006).
- <sup>10</sup>R. A. Senter, C. Pantea, Y. Wang, H. Liu, T. W. Zerda, and J. L. Coffey, *Phys. Rev. Lett.* **93**, 175502 (2004).
- <sup>11</sup>Q. Xu, I. D. Sharp, C. W. Yuan, D. O. Yi, C. Y. Liao, A. M. Glaeser, A. M. Minor, J. W. Beeman, M. C. Ridgway, P. Kluth, J. W. Ager III, D. C. Chrzan, and E. E. Haller, *Phys. Rev. Lett.* **97**, 155701 (2006).
- <sup>12</sup>*CRC handbook of Chemistry and Physics*, edited by D. R. Lide (CRC, Boca Raton, FL, 2006).
- <sup>13</sup>G. H. Dieke, *Spectra and Energy Levels of Rare Earth Ions in Crystals* (Interscience, New York, 1968).
- <sup>14</sup>M. Perálvarez, J. Carreras, J. Barreto, A. Morales, C. Domínguez, and B. Garrido, *Appl. Phys. Lett.* **92**, 241104 (2008).
- <sup>15</sup>A. Nazarov, J. M. Sun, W. Skorupa, R. A. Yankov, I. N. Osiyuk, I. P. Tjagulskii, V. S. Lysenko, and T. Gebel, *Appl. Phys. Lett.* **86**, 151914 (2005).
- <sup>16</sup>M. C. Ridgway, G. de M. Azevedo, R. G. Elliman, C. J. Glover, D. J. Llewellyn, R. Miller, W. Wesch, G. J. Foran, J. Hansen, and A. Nylandsted-Larsen, *Phys. Rev. B* **71**, 094107 (2005).
- <sup>17</sup>L. Pavesi and M. Ceschini, *Phys. Rev. B* **48**, 17625 (1993).
- <sup>18</sup>I. Izuddin, A. S. Moskalenko, I. N. Yassievich, M. Fujii, and T. Gregorkiewicz, *Phys. Rev. Lett.* **97**, 207401 (2006).